Control of Hybrid AC/DC Microgrid Involving Energy Storage, Renewable Energy and Pulsed Loads

Tan Ma, Mehmet Hazar Cintuglu, Student Members, IEEE, Osama Mohammed, Fellow, IEEE

***Abstract*—This paper proposes the coordinated control of a hybrid AC/DC power system with renewable energy source, energy storages and critical loads. The hybrid microgrid consists of both AC and DC sides. A synchronous generator and a PV farm supply power to the system's AC and DC sides, respectively. A bidirectional fully controlled AC/DC converter with active and reactive power decoupling technique is used to link the AC bus with the DC bus while regulating the system voltage and frequency. A DC/DC boost converter with a maximum power point tracking (MPPT) function is implemented to maximize the energy generation from the PV farm. Current controlled bidirectional DC/DC converters are applied to connect each lithium-ion battery bank to the DC bus. Lithium-ion battery banks act as energy storage devices that serve to increase the system stability by absorbing or injecting power to the grid as ancillary services. The proposed system can function in both grid-connected mode and islanding mode. Power electronic converters with different control strategies are analyzed in both modes in detail. Simulation results in MATLAB Simulink verify that the proposed topology is coordinated for power management in both AC and DC sides under critical loads with high efficiency, reliability, and robustness under both grid-connected and islanding modes.**

***Index Terms*—Ancillary services, battery bank, critical load, energy management, hybrid AC/DC power system, micro grid, solar energy.**

I. INTRODUCTION

HYBRID power systems are growing in popularity due to the increase in microgrid implementing renewable power conversion systems connected to low voltage AC distribution systems. This growth has also been attributed to the environmental issues caused by conventional fossil fueled power plants [1]-[3]. Furthermore, DC grids are resurging due to the development of new semiconductor techniques and sustainable DC power sources such as solar energy. There has also been an increase in DC loads, such as plug-in electric vehicles (PEVs) and light emitting diodes (LEDs), connected to the grid to save energy and decrease greenhouse gas emissions. The PEVs can be viewed as energy storage devices when they are parked in the garage, allowing them to increase the stability and efficiency of the micro grid they are connected to. One of the major technical challenges in micro grids is the interconnection of a pulse load which can cause voltage collapse, oscillation of the angular velocity in the generators, and degradation of the overall system performance.

Researchers have proposed several ideas and models relating to renewable energy sources and storage, ranging from their scheduling and PEV charging optimizations to the feasibility of PEV vehicle-to-grid (V2G) services[4]-[6]. However, these models only propose the idea without thorough analysis of the of the energy conversion between the AC and DC sides. Researchers have also proposed several ideas and models of AC/DC micro grids [7]-[9], but their systems operate without the influence of the critical loads. System stability and coordination control of power electronics devices during grid-connected and islanding modes with the influence of critical loads is still an open issue.

At the same time, various utility grids and some hybrid microgrids are increasing the penetration of renewable energy resources [10]-[11]. This growth in renewable sources increased the challenge these systems will meet due to the intermittent nature of wind and solar power. This can quickly add up to system-wide instability that can force generators to ramp up and down wildly, push grid protection gear into states it's not meant to handle, or force the wind and solar generator to shut off altogether [12] . Hybrid power systems face far more challenges when operating in islanding mode than they do in grid connected mode. During islanding mode, the AC side can no longer be viewed as an infinite bus, which results in load variations adversely affecting the frequency and voltage of the system. If the system has a high penetration of renewable power, the situation can be even worse. At any time, power flow should be balanced between the AC and DC sides to maintain stability on both sides of the grid. Also, both reactive and active power in the AC side of the system should be balanced to keep the frequency and voltage stable.

In this paper, a hybrid AC/DC micro grid with solar energy, energy storage, and pulse load is proposed. This micro grid can be viewed as a PEV parking garage power system or a ship power system that utilizes sustainable energy and is influenced by pulse load. The system operation and power converters coordination control are studied in both grid-connected and islanding model. The power flow control of these devices serves to increase the system's efficiency, stability, and robustness. This paper is organized as follows; system configuration and modeling of the PV farm and battery banks are presented in Section II. Coordinated control strategies for the converters in grid-connected mode and islanding mode are presented in Section III. Section IV demonstrates the simulation results that verify the proposed topology and control method can increase system stability and efficiency under the influence of a pulse load. Finally, conclusions are drawn in Section V.

Part of this work was sponsored by the Office of Naval Research. The authors are with the Energy Systems Research Laboratory, Department of Electrical and Computer Engineering, Florida International University, Miami, FL 33174 USA (e-mail: mohammed@fiu.edu).

Add the wind generator

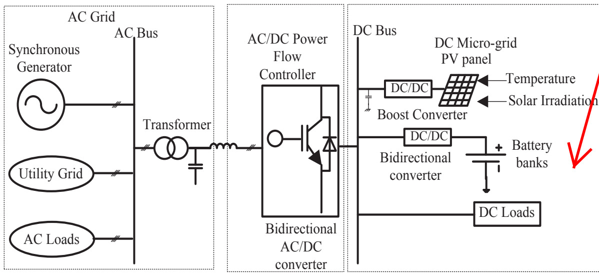

Fig. 1 Hybrid AC-DC microgrid power system.

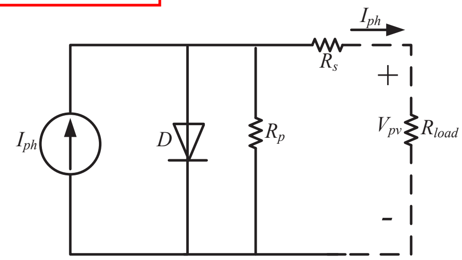

Fig. 3 Equivalent circuit of a PV panel

II. System Configuration and Modeling

A. Grid Configuration

Fig. 1 shows the hybrid micro grid configuration where a synchronous generator, a PV farm, and loads are connected to its corresponding AC and DC sides. The AC and DC sides are linked through a bidirectional three phase AC/DC converter and a transformer. The system has constant loads and pulse loads in both AC and DC sides. The 10kW PV farm is connected to the DC bus as the DC energy source through a DC/DC boost converter with MPPT functionality. A synchronous three phase generator with 13.8kVA capacity and 208V phase-phase rms terminal voltage is connected to the AC side. Five 50Ah lithium-ion battery banks with 51.8V terminal voltage are connected to the DC bus through five bidirectional DC/DC boost converters. The rated voltages for DC and AC sides are 300V and 208V phase to phase rms respectively. A 10 kW pulse load is connected to AC and DC sides respectively.

The system can be operated in either grid-connected mode or islanding mode. To maximize the utilization of the renewable sources, the PV panel is working in maximum power point in both modes by controlling the DC/DC boost converter. In grid-connected mode, the proposed system can be viewed as a PEVs car park system. The five batteries can be viewed as five PEVs that can play the role of energy storage devices [5]. By controlling the charging process of the PEVs in the car park, the hybrid micro grid can limit the PEVs' charging impact to the utility grid and at the same time provide some ancillary supports to the utility grid through V2G services, including frequency regulation, reactive power compensation, spinning reserve, and so on. The detail of the car park configuration is shown in Fig. 2. In islanding mode, the proposed system can be viewed as a ship power system with solar panels. The bi-directional AC/DC converter will take charge of the AC side frequency and voltage amplitude. The DC bus voltage is regulated by controlling the charging and discharging of the battery banks, which also means controlling the current flow through the bi-directional DC/DC converter.

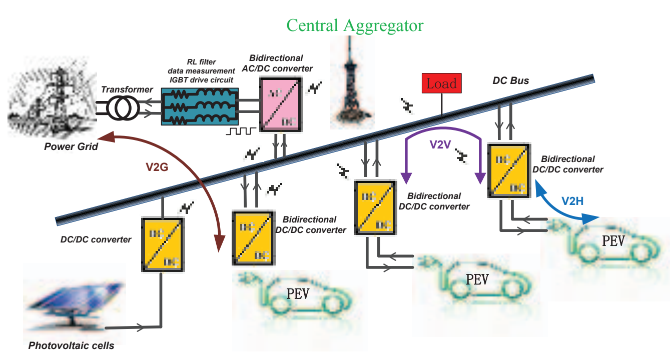

Fig.2 Hybrid PEVs car park power system.

TABLE I
PARAMETERS FOR PHOTOVOLTAIC PANEL

Symbol	Description	Vaule
V_{oc}	Rated open circuit voltage	$64.2\ V$
I_{ph}	Photocurrent	$5.9602\ A$
I_{sat}	Module reverse satuation current	1.1753×10^{-8}
q	Electron charge	$1.602\times10^{-19}\ C$
A	Ideality factor	1.50
k	Boltzman constant	$1.38\times10^{-23}\ J/K$
R_s	Series resistance of a PV cell	$0.037998\ \Omega$
R_p	Parallel resistance of a PVcell	$993.51\ \Omega$
I_{sso}	Short-circuit current	$5.96\ A$
k_i	SC current temperature coefficient	1.7×10^{-3}
T_r	Reference temperature	$301.18\ K$
I_{rr}	Reverse saturation current at T_r	$2.0793\times10^{-6}\ A$
E_{gap}	Energy of the band gap for silicon	$1.1eV$
n_p	Number of cells in parallel	528
n_s	Number of cells inseries	480
S	Solar radiation level	$0\sim1000\ W/m^2$
T	Surface temperature of the PV	$350\ K$

B. Modeling of PV Panel

The PV panel can be viewed as a current source in parallel with a diode. Fig. 3 shows the equivalent circuit of a PV panel with a load. In this paper, the SunPower SPR-305-WHT solar cell with 305W maximum output power is used. 33 cells are used with the configuration of 11 parallel strings, and 3 serially connected cells per string. Fig. 4 shows the non-linear P-V and I-V electric characteristics of a single SunPower

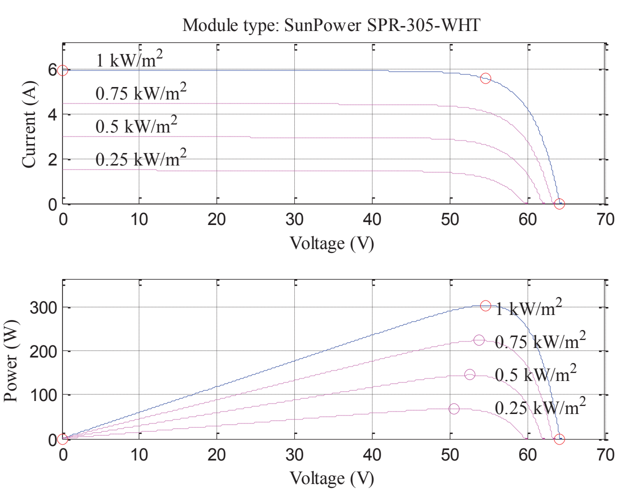

Fig. 4 I-V and P-V curves for PV panel Sumpower SPR-305-WHT

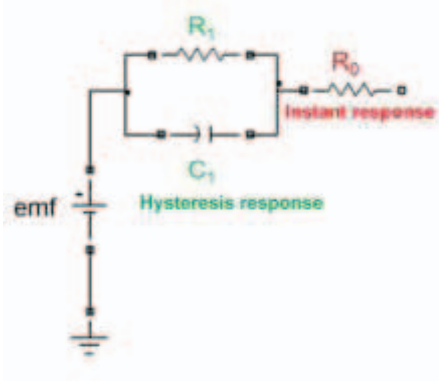

Fig. 5 Lithium-ion battery equivalent circuit

SPR-305-WHT solar sell. It is clear that under different solar irradiations, the maximum power points of the power-voltage curves are associated with different output voltages. Also, under certain solar irradiance, the output of the PV panel is varying with different terminal voltages. Equations (1)-(3) show the mathematical model of the PV panel and its output current [13]. All the parameters are shown in Table I.

$$I_{pv} = n_p I_{ph} - n_p I_{sat} \cdot [\exp((\frac{q}{AkT})(\frac{V_{pv}}{n_s} + I_{pv}R_s)) - 1] \quad (1)$$

$$I_{ph} = (I_{sso} + ki(T - T_r)) \cdot \frac{S}{1000} \quad (2)$$

$$I_{sat} = I_{rr}(\frac{T}{Tr})^3 \exp((\frac{qE_{gap}}{kA}) \cdot (\frac{1}{T_r} - \frac{1}{T})) \quad (3)$$

C. Modeling of Lithium-ion Battery Bank

An accurate battery cell model is needed to regulate the DC bus voltage in islanding mode. The battery terminal voltage and SOC need to be estimated during operation. A high fidelity electrical model of lithium-ion battery model with thermal dependence is used [14]. The equivalent circuit of the battery model is shown in Fig. 5. The instantaneous response is modeled by a resistor R_0 and the hysteresis response is modeled by a non-linear RC circuit R_1 and C_1. E_{mf} represents the internal voltage of the battery. All four parameters are related to different SOCs and temperatures, so four lookup tables are established by using the parameter estimation toolbox in Simulink Design Optimization for these four parameters under different circumstances. The flow diagram of the parameter estimation procedure is shown in Fig. 6. The SOC of each single battery cell can be calculated by equation (4).

$$SOC = 1 - \frac{Q_e}{C_Q} \quad (4)$$

Where Q_e is extractable charge and C_Q is the total capacity of the cell. Below is the equation (5) for extractable charge Q_e of an individual cell along with the total capacity of the cell which is dependent on current and temperature.

$$Q_e(t) = \int_0^t I_m(\tau)d\tau \quad (5)$$

$$C_Q = C_Q(I,T) \quad (6)$$

D. Modeling of Critical Load

The pulse load can be connected to both the AC and DC side. On the DC side, the pulse load can usually be viewed as a pure resistive load. On the AC side, the pulse load can be either resistive load or inductive load, such as an induction motor. However, those inductive loads are commonly connected to the AC side through the power electronic drivers, such as the back to back converters. In this way, the inductive load can be converted and acted as a resistive load. Therefore, in this paper, only resistive loads are used to emulate the performance of critical load.

III. Coordinated Control of the Converters

Three types of converters are utilized in this proposed hybrid microgrid. These converters must be actively controlled in order to supply uninterrupted power with high efficiency and quality to critical loads on the AC and DC sides during grid-connected and islanding modes. The cooperated control strategies for the converters are discussed in this section.

A. Boost Converter Control with MPPT

To maximize the utilization of renewable energy from the PV farm, the boost converter should be operated in on-MPPT mode when the hybrid microgrid is connected to the utility grid. The battery banks or the PEVs in the microgrid can be used as an energy buffer, and the charging/discharging rates can be controlled based on the status of the output power from the PV farm and the power flow in the AC side. In islanding mode, the

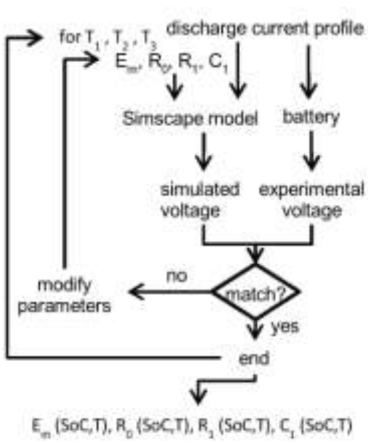

Fig. 6 Flow diagram of the parameter estimation procedure.

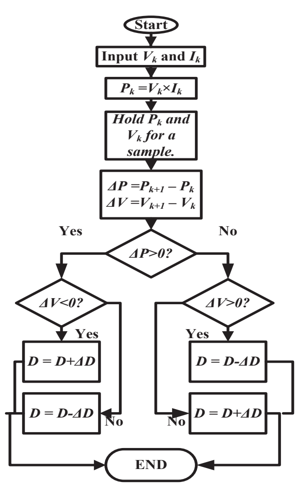

Fig. 7 Flow chart of P&O MPPT method

boost converter of the PV farm can be operated in on-MPPT or off-MPPT which is based on the system's power balance and the SOCs of the battery banks. In most situations, this boost converter can operate in the on-MPPT mode since the variation ratio of the solar irradiance is much lower compared with the power adjustment ability of the small size AC generator. Therefore, for a constant load either on the AC or DC side, the PV should supply as much power as possible to maximize its utilization. However, if the battery banks' SOCs are high (near fully charged) and the PV's maximum output power is larger than the total load in the hybrid microgrid, the PV should be turned to off-MPPT to keep the system power in balance.

In this paper, the perturbation and observe (P&O) method is used to track the maximum power point. The algorithm utilizes the PV farm output current and voltage to calculate the power. The values of the voltage and power at the k^{th} iteration (P_k) are stored, then the same values are measured and calculated for the $(k+1)^{th}$ iteration (P_{k+1}). The power difference between the two iterations (ΔP) is calculated. The converter should increase the PV panel output voltage if ΔP is positive and decrease the output voltage if ΔP is negative, which finally will adjust the duty cycle. The PV panel reaches the maximum power point when ΔP is approximately zero. The flow chart of the P&Q MPPT algorithm is given is Fig. 7.

B. Bi-Directional DC/DC Converter Control

The bi-directional DC/DC converters are used to connect the battery banks to the DC bus. In grid-connected mode, those converters only regulate the battery banks (or PEVs) charging rates. Based on the SOCs of the battery banks and the power flow conditions in the AC side, the charging/discharging current references are generated to regulate the current flow in the converters. Each battery has its own bi-directional DC/DC converter, which means they can have different charging rates. By doing this, the battery banks can inject power to or absorb power from the DC bus, and even transfer energy between different battery banks if necessary. In this case, only one current control close loop with PI controller is enough to regulate the current.

The bi-directional DC/DC converters of the battery banks play an important role in islanding mode to regulate the DC bus voltage. A two-loops control is used to regulate the DC bus voltage. The control scheme for the bi-directional DC/DC converter is shown in Fig. 8. The outer voltage controlled loop is used to generate a reference charging current for the inner current controlled loop. The error between the measured DC bus voltage and the system reference DC bus voltage is set as the input of the PI controller, and the output is the reference current. The inner current control loop will compare the reference current signal with the measured current flow through the converter and finally generate a PWM signal to drive the IGBTs to regulate the current flow through the converter. For example, when the DC bus voltage is higher than the reference voltage, the outer voltage controller will generate a negative current reference signal, and the inner current control loop will adjust the duty cycle to force the current flow from the DC bus to the battery, which results in charging of the battery. In this way, the energy transfers from the DC bus to the battery and the DC bus voltage will decrease to the rating value. If the DC bus voltage is lower than the normal value, the outer voltage control loop will generated a positive current reference signal, which will regulate the current flow from the battery to the DC bus, and because of the extra energy injected from the batteries, the DC bus voltage will increase to the rating value. All five batteries and their bi-directional converters are coordinated together to regulate the DC bus voltage. The battery SOC and thermal self-balancing control can be applied to protect the battery banks from over discharge and overheating [15].

C. Bi-directional AC/DC converter control

In d-q coordinates, I_d is controlled to regulate the active power flow through the inverter, and I_q is controlled to regulate the reactive power flow through the inverter. In the AC side, the active and reactive power flow will influence the frequency and voltage amplitude respectively.

In grid-connected mode, the AC side can be viewed as an infinite bus. Therefore the variances of the voltage amplitude and frequency can be ignored. In this case, the bi-directional AC/DC converter only needs to regulate the DC bus voltage. In order to operate in unit power factor, reference i_q can be set as 0. The controller only need to control the i_d, which in the end will control the active power flow through the converter. What's more, if the grid needs the microgrid to provide ancillary services, such as V2G frequency regulation, the proposed configuration is also qualified. For example, when the system

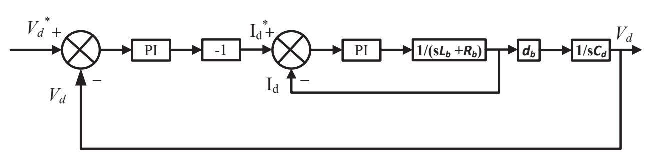

Fig.8. The control block diagram for bi-directional DC/DC converter

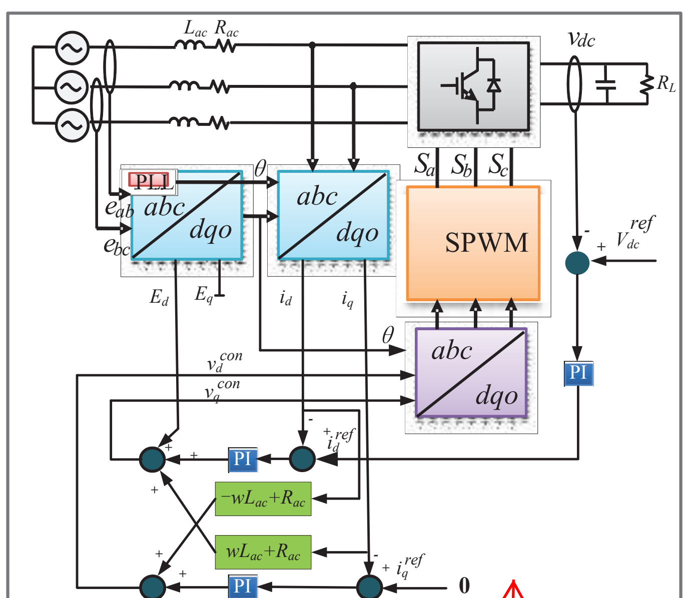

Fig.9. The control block diagram for bi-directional AC/DC converter in grid-connected mode

DPC of rectifier with outer voltage loop

MPC of inverter with grid voltage as the control objective of the cost function

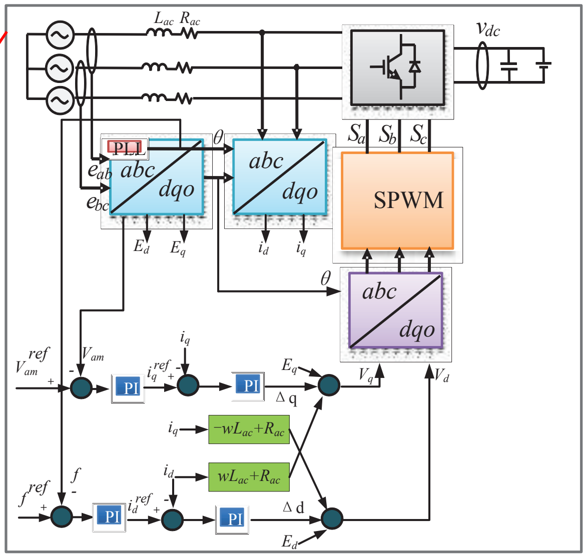

Fig.10. The control block diagram for bi-directional AC/DC converter in islanding mode

frequency is below 60 Hz, then the central control aggregator in Fig. 2 will send a command to the bi-directional DC/DC converter to let the PEVs inject power to the DC bus. The excess energy being generated from the PEVs will result in an increase in the DC bus voltage. The bidirectional AC/DC converter will sense this voltage increase and will decrease the current reference, i_d. This decrease in current reference will result in the decrease of active power flow from the AC side to the DC side of the micro grid. If i_d decreases to a negative value, then energy will be transferred from the DC side to the AC side. In the end, the power is balanced in the AC side, and the frequency will increase back to 60 Hz. The control block diagram for bi-directional AC/DC converter in grid-connected mode is shown in Fig. 9. A two loop controller is used to regulate the DC bus voltage. Based on the error between the DC bus reference voltage and measured voltage, the outer voltage control loop generates the i_d reference which is used to regulate i_d in the bi-directional converter.

In islanding operation mode, the frequency and voltage amplitude of the three phases AC side are not so robust, therefore a device is needed to regulate them. The bi-directional AC/DC inverter is used to regulate the active and reactive power by controlling the i_d and i_q respectively. The Control scheme for the bi-directional AC/DC inverter is shown in Fig. 10. Two-loop controllers are applied for both frequency and voltage regulation. For frequency control, error between measured frequency and reference frequency is sent to a PI controller which generates the i_d reference. To control the voltage amplitude, the error between the measured voltage amplitude and the reference voltage amplitude is sent to a PI controller to generate i_q reference. Equations (7) and (8) show the AC side voltage equations of the bi-directional AC/DC inverter in ABC and d-q coordinates, respectively. Where (V_a, V_b, V_c) are AC side voltages of the inverter, and (E_a, E_b, E_c) are the voltages of the AC bus. (Δ_a, Δ_b, Δ_c) are the adjusting signals after the PI controller in the current control loop.

$$L_{ac}\frac{d}{dt}\begin{bmatrix} i_a \\ i_b \\ i_c \end{bmatrix} + R_{ac}\begin{bmatrix} i_a \\ i_b \\ i_c \end{bmatrix} = \begin{bmatrix} V_a \\ V_b \\ V_c \end{bmatrix} - \begin{bmatrix} E_a \\ E_b \\ E_c \end{bmatrix} + \begin{bmatrix} \Delta_a \\ \Delta_b \\ \Delta_c \end{bmatrix} \tag{7}$$

$$L_{ac}\frac{d}{dt}\begin{bmatrix} i_d \\ i_q \end{bmatrix} = \begin{bmatrix} -R_{ac} & \omega L_{ac} \\ -\omega L_{ac} & -R_{ac} \end{bmatrix}\begin{bmatrix} i_d \\ i_q \end{bmatrix} + \begin{bmatrix} V_d \\ V_q \end{bmatrix} - \begin{bmatrix} E_d \\ E_q \end{bmatrix} + \begin{bmatrix} \Delta_d \\ \Delta_q \end{bmatrix} \tag{8}$$

When the pulse load is connected or disconnected to the AC side, the frequency or the voltage amplitude will be altered. After detecting the variance from the phase lock loop (PLL) or voltage transducer, I_d and I_q reference signals will be adjusted to regulate power flow through the bi-directional AC/DC inverter. Because of the power flow variances, the DC bus voltage will also be influenced. The DC bus voltage transistor will sense the voltage variance in DC bus, and the bi-directional DC/DC converter will regulate the current flow between the battery and the DC bus. In the end, the energy is transferred between the battery and the AC side to balance the power flow in the system.

IV. System Simulation Results

The operations of the hybrid micro grid utilizing a 10.07 kW PV farm under the influence of a 10 kW pulse load is simulated to verify the proposed hybrid microgrid. The rated power of the synchronous generator is 13.8 kW, and a 4 kW constant load is connected in the AC side. Five 51.8V 21Ah Lithium-ion battery banks are connected individually to the DC bus through bidirectional DC/DC converters. The MATLAB Simulink model of the proposed system is shown in Fig. 11. The system parameters for the hybrid micro grid are listed in Table II. The main operation differences between the grid-connected mode and the islanding mode are the control of the bi-directional AC/DC converter and the bi-directional DC/DC converter. The operations of the boost converter which connects the PV farm and the DC bus in both modes are same. Therefore, the

TABLE II
Hybrid Microgrid System Parameters

Symbol	Description	Vaule
C_{pv}	Solar panel capacitor	100 uF
L_{pv}	Inductor for solar Panel boost converter	5mH
C_d	DC bus capacitor	6000 uF
L_{ac}	AC filter inductor	1.2mH
R_{ac}	Inverter equivalent resistance	0.3ohm
L_b	Battery converter inductor	3.3mH
R_b	Resistance of L_b	0.5 Ω
f	Rated AC grid frequency	60Hz
V_d	Rated DC bus voltage	300V
Vm	Rated AC bus p-p voltage (rms)	208K
$n1/n2$	Transformer ratio	1:1

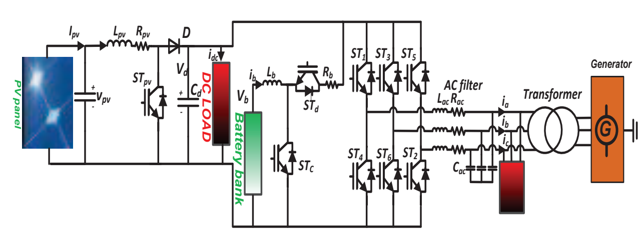

Fig. 11 The compact Matlab Simulink model of the proposed micro grid

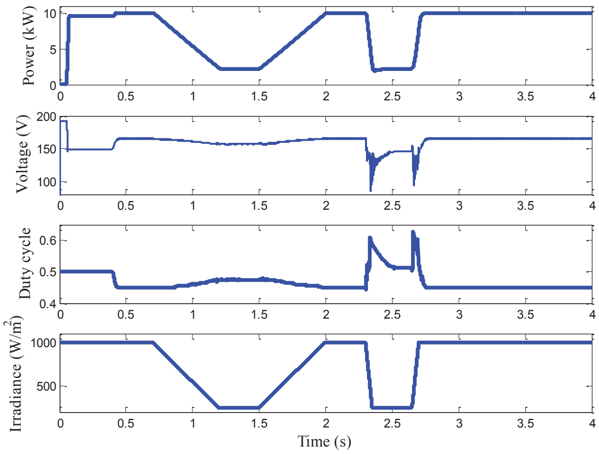

Fig. 12 PV farm output power control with MPPT.

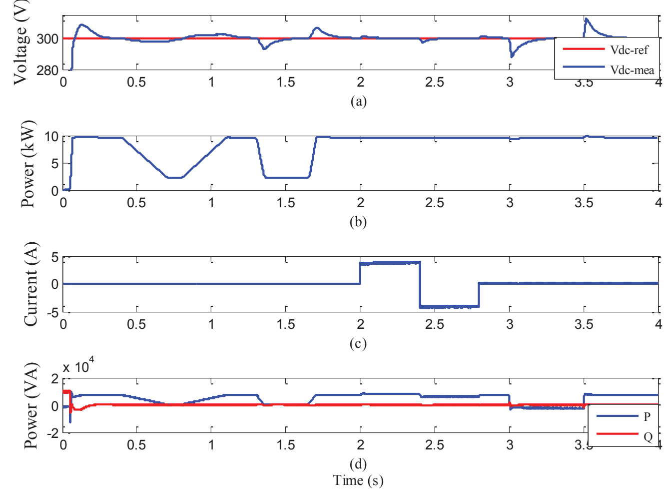

Fig. 13 Hybrid micro grid performance in grid-connected mode.

performance of the boost converter is discussed fist.

In both grid-connected mode and islanding mode, to maximize the utilization of renewable energy, the boost converter is working in on-MPPT mode to keep seeking the maximum output power from the PV farm. The MPPT of the boost converter is enabled at 0.4s. The output power, the terminal voltage of the PV panel, the duty cycle of the boost converter and the solar irradiance are shown in Fig. 12. For general study, two kinds of solar irradiance variances with different charging rates are used in this study. Before 0.4s, the duty cycle is set at 0.5, the terminal voltage of the PV panel is 149V and the output power from the PV panel is only 9.56 kW. After the MPPT is enabled, the duty cycle is decreased to 0.45. The terminal voltage is increased to 165V. This allows the PV panel to reach the maximum power output of 10.07 kW. The simulation results show that the boost converter with MPPT functionality can track the maximum power point within a short response time.

A. Grid-connected Mode

In grid-connected mode, the DC bus voltage is regulated by the bi-directional AC/DC converter. In this mode, the AC side can be viewed as infinite bus, therefore the 10 kW resistive pulse load that is connected to the AC side will not have an influence on the grid. Therefore, only the DC pulse load case is studied. The system performance with the influence of the PV output power variance and battery banks (PEVs) charging rate variance is shown in Fig. 13. Fig 13 (a) shows the DC bus voltage. The bi-directional AC/DC converter was enabled at 0.05s. Before that, it operated as an uncontrolled rectifier. After enabling the bi-directional converter, the DC bus voltage reached steady state in less than 0.3s. During this period, the solar irradiance is 1kW/m^2. From 0.4s to 1.7s, system under two kinds of solar irradiance variations is simulated. The output power from PV decreased from 10kW to 2.5kW in 0.3 second and recovered back from 2.5kW to 10kW also in 0.3 second. After that, the PV output decreased from 10kW to 2.5 kW in 0.05 second at 1.3s and went back from 2.5kW to 10kW at 1.65s. The PV output power is shown in Fig. 13 (b). The DC bus voltage was stable and kept in the range of 293V to 307V during this process, the bi-directional converter can keep the DC side stable under rapid alteration of solar irradiance and PV output power. From 2s to 2.8s, the charging/discharging of battery banks impact to the DC bus is simulated. This process can be viewed as the study of the PEVs charging process in reference [5]. At 2s, the current references of the bi-directional DC/DC converters of those five batteries were changed from 0A to -4A, which means discharging those battery banks with 4A. At 2.4 seconds, the current references of the bi-directional DC/DC converters of the five battery banks were changed from 0A to 4A, and the system began charging the battery banks. The current flow of one bi-direction DC/DC converter is shown in Fig. 13 (c). During this period, the DC bus voltage was still stable with less than 3V voltage variance. From 3s to 3.5s, a 10kW resistive load is connected to the DC bus. During the connection and disconnection of the 10 kW pulse load, the bi-directional AC/DC inverter active power flow was greatly changed to regulate the DC bus voltage. The DC bus was still stable within 12V voltage variance during the transient response.

The power flow through the bi-directional AC/DC inverter is shown in Fig. 13 (d). After the system entered steady state, the system kept unit power factor as the reactive power was 0. The active power flow varied with the solar irradiance influence, battery banks charging/discharging influence and pulse load influence. The bi-directional inverter can quickly adjust the power flow through it and keep the microgrid in stable.

B. Islanding Mode

During islanding mode operation, the frequency and voltage amplitude need to be regulated. Usually, the generator in the microgrid can handle the load with a small varying ratio, but when the pulse load is connected to the AC side or the total load exceeds the generator's limit, the system frequency may decrease and the voltage may collapse. Therefore, the bidirectional AC/DC inverter is used to regulate the AC side frequency and voltage amplitude.

In this case study, the AC side has a 4kW constant resistive load, and a 10kW pulse resistive load is connected from 2.2s to 2.8s. After that, a 10kW pulse resistive load is connected to the DC bus during 3.3s to 3.8s.

Fig. 14 (a) shows the DC bus voltage with the influence of

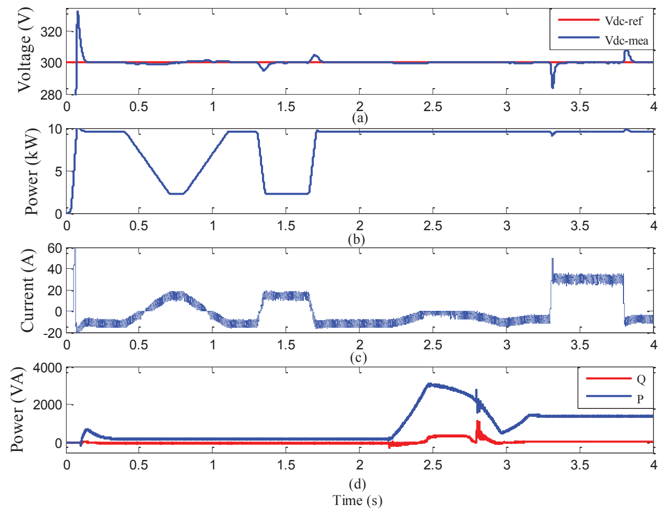

Fig. 14 Hybrid micro grid performance in islanding mode.

solar irradiance variation on the PV panels and the pulse load connected in the AC side and DC side. The bidirectional DC/DC converter was enabled at 0.05s to regulate the DC bus voltage, and the DC bus voltage reached the steady state in less than 0.2 seconds. The PV farm output power variance is shown in Fig. 14 (b). When the 10kW pulse load is connected to the DC bus, those five battery banks cooperated together to regulate the voltage, therefore the DC bus voltage kept stable with a maximum variance of 17V during the transient response, the current follow through one bi-directional DC/DC converter is shown in Fig. 14 (c). The AC side pulse load connection and disconnection did not greatly impact the DC bus voltage since the battery banks have enough energy to support and balance the power flow with a quick response. The bi-directional AC/DC inverter successfully transferred the energy from the battery banks to the AC side when the pulse load happened. The active and reactive power flow through the bi-directional AC/DC inverter is shown in Fig. 14 (d).

Fig. 15. (a) and (b) show the AC bus voltage and current. The AC bus voltage transient response during the pulse load connection is shown in Fig. 15 (a). The AC voltage amplitude returned to its normal value in less than three cycles. When the

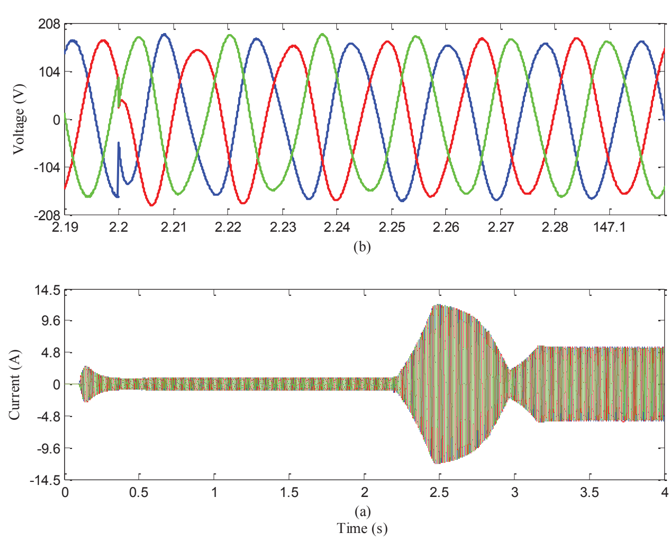

Fig. 15 Microgrid AC bus voltage and current response with DC support.

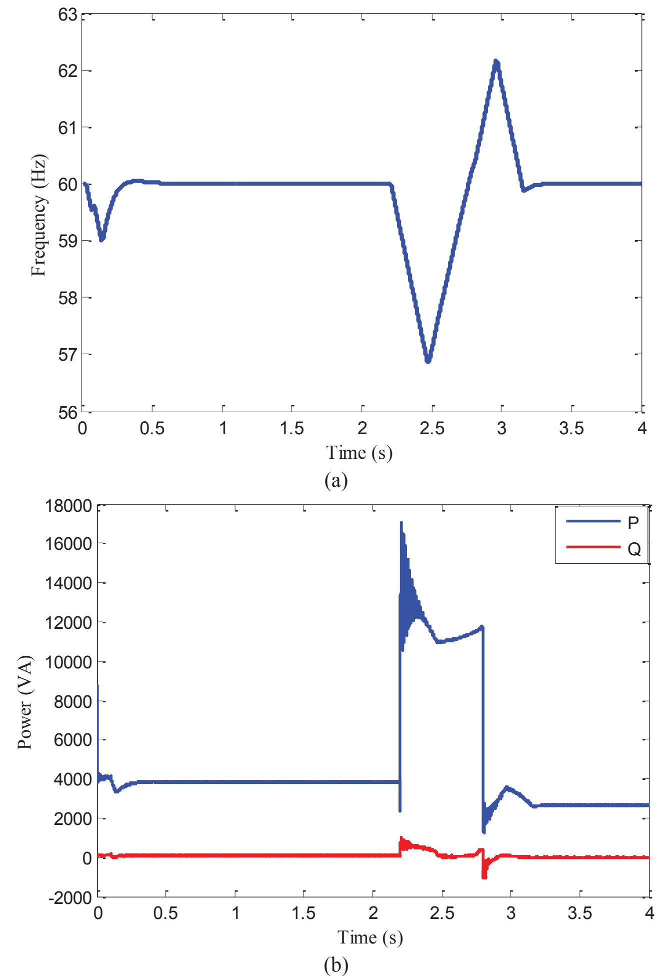

Fig.16 Microgrid AC side pulse load response with DC support.

pulse load was connected to the AC side, the current flow through the AC bus increased immediately, and after the pulse load disconnected from the AC side, the current slightly decreased to keep the system in balance. The current flow through AC bus is shown in Fig. 15(b).

Fig. 16 (a) shows the AC side frequency variation. The AC/DC bi-directional inverter was enabled at 0.1s and the AC side frequency was stable at 60 Hz in less than 0.4 second. When the resistive pulse load was connected at t=2.2s, the frequency dropped to 58 Hz and returned to 60 Hz in less than 1 second. When the pulse load was disconnected from the AC side, the frequency increased to 62 Hz and returned to stead state in less than 0.5s. The power generated from the generator is shown in Fig.16 (b). The hybrid microgrid is stable in both its AC and DC side.

Another simulation was done for the hybrid micro grid under same islanding mode operation without DC side support. When the 10 kW resistive pulse load was connected to the AC bus, the total load in the AC side was 14 kW which exceeded the generator's output limitation by 0.2 kW. Fig. 17 (a), (b) and (c) shows the AC side generator's voltage, current and output power. The pulse load was connected to the AC side at 2s, after 0.2 second the system collapsed, and both the frequency and voltage dropped considerably. The system couldn't recover even the pulse load was disconnected after t=3s.

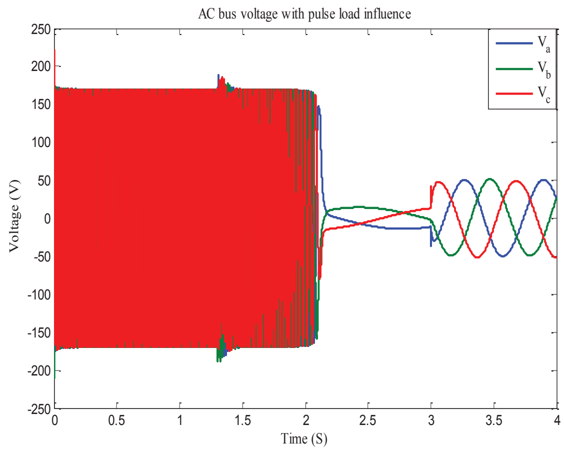

(a)

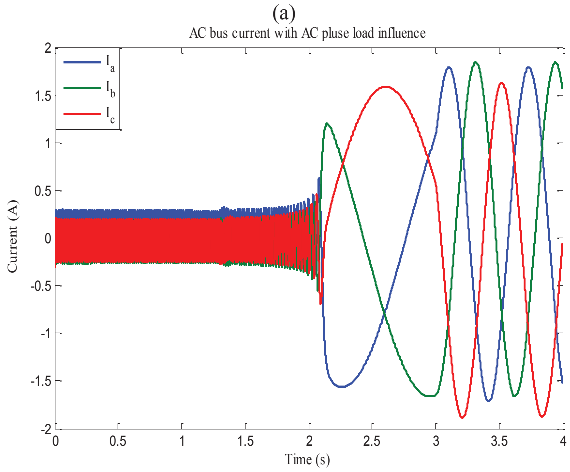

(b)

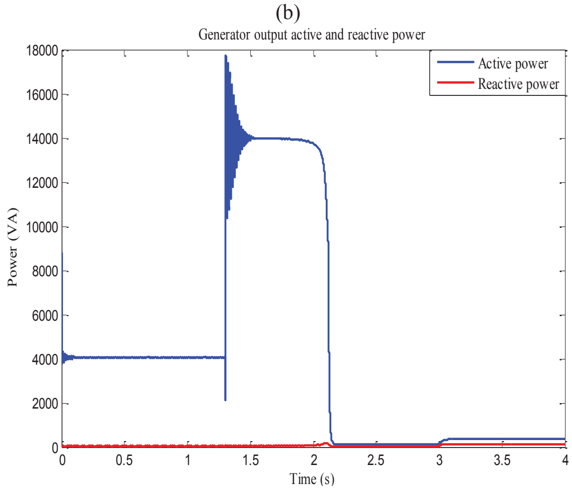

(c)

Fig. 17 Microgrid AC side pulse load response without DC support.

V. Conclusion

In this paper, a coordination power flow control method of multi power electronic devices is proposed for a hybrid AC/DC microgrid operated in both grid-connected and islanding modes. The microgrid has a PV farm and a synchronous generator that supply energy to its DC and AC side. Battery banks are connected to the DC bus through bi-directional DC/DC converter. The AC side and DC side are linked by the bi-directional AC/DC inverter. The system topology together with the control algorithms under both modes are tested with the influence of pulse loads and renewable energy farm output power variances. The simulation results show that the proposed microgrid with the control algorithm can greatly increase the system stability and robustness.

References

[1] C. K. Sao and P. W. Lehn, "Control and power management of converterfed MicroGrids," *IEEE Trans. Power Syst*., vol. 23, no. 3, pp. 1088–1098, Aug. 2008

[2] A. Mohamed, F. Carlos, T. Ma, M. Farhadi, O. Mohammed, "Operation and protection of photovoltaic systems in hybrid AC/DC smart grids," *IECON* 2012 – 38th Annual Conference on *IEEE Industrial Electronics Society*, pp.1104-1109, 25-28 Oct. 2012

[3] R. H. Lasseter and P. Paigi, "Microgrid: A conceptual solution," in Proc. *IEEE* 35th *PESC*, Jun. 2004, vol. 6, pp. 4285–4290.

[4] C. Liu, K.T. Chau, D. Wu, and S. Gao, "Opportunities and challenges of vehicle-to-home, vehicle-to-vehicle and vehicle-to-grid technologies," *Proceeding of the IEEE, Invited Paper*, vol. 101, no. 11, pp. 2409-2427, Nov. 2013.

[5] T. Ma, and O. Mohammed. "Optimal charging of plug-in electric vehicles for a car park infrastructure," to be published on *IEEE Trans. Industry Applications*, July. 2014.

[6] T. Ma, O. Mohammed,. "Economic analysis of real-time large scale PEVs network power flow control algorithm with the consideration of V2G services. " In Industry Applications Society Annual Meeting, 2013 IEEE (pp. 1-8).

[7] X. Liu, P. Wang and P. C. Loh, "A Hybrid AC/DC Microgrid and Its Coordination Control," *IEEE Trans. Smart Grid* , vol.2, no.2, pp.278,286, June 2011.

[8] V. Salehi, A. Mohamed, A. Mazloomzadeh, O.A.Mohammed, "Laboratory-Based Smart Power System, Part II: Control, Monitoring, and Protection", *IEEE Trans*, *Smart Grid*, Sept. 2012, vol. 3, no.3, pp 1405-1417

[9] A. Mohamed, V. Salehi and O. Mohammed, "Reactive Power Compensation in Hybrid AC/DC Networks for Smart Grid Applications," in Proc. *Innovative Smart Grid Technologies Conf*., *ISGT* Europe 2012, Berlin, Germany, October 14-17, 2012

[10] M. Schuerger, H. Johal, L. Roose, M. Matsuura,and R. Piwko, "Catching Some Rays: Variable Generation Integration on the Island of Oahu," *Power and Energy Magazine, IEEE* , vol.11, no.6, pp.33,44, Nov. 2013

[11] M. Ahlstrom, et al "Knowledge Is Power: Efficiently Integrating Wind Energy and Wind Forecasts," *Power and Energy Magazine, IEEE* , vol.11, no.6, pp.45,52, Nov. 2013

[12] N. Miller, C.Loutan, Shao Miaolei, K. Clark, "Emergency Response: U.S. System Frequency with High Wind Penetration, " *Power and Energy Magazine, IEEE* , vol.11, no.6, pp.63,71, Nov. 2013

[13] M. E. Ropp and S. Gonzalez, "Development of a MATLAB/simulink model of a single-phase grid-connected photovoltaic system," IEEE Trans. Energy Conv., vol. 24, no. 1, pp. 195–202, Mar. 2009.

[14] T. Huria, M. Ceraolo, J. Gazzarri, R. Jackey, "High fidelity electrical model with thermal dependence for characterization and simulation of high power lithium battery cells," *Electric Vehicle Conference (IEVC)*, *IEEE International* pp.1,8, 4-8 March 2012

[15] H. Rahimi-Eichi, U. Ojha, F. Baronti, M. Chow, "Battery Management System: An Overview of Its Application in the Smart Grid and Electric Vehicles, " *Industrial Electronics Magazine, IEEE* , vol.7, no.2, pp.4,16, June 2013.